COMPARATIVE ANALYSIS OF WORKING FLUIDS IN SOLAR JOULE BRAYTON COGENERATION ENGINES

Gheorghe DUMITRAŞCU[1], Michel FEIDT[2], Bogdan HORBANIUC[1]

[1]GHEORGHE ASACHI TECHNICAL UNIVERSITY OF IASI, Romania.
[2] ENSEM-LEMTA, UNIVERSITY HENRI POINCARÉ OF NANCY, France.

Rezumat. Lucrarea include o analizã comparativã a influenţei naturii agentului de lucru asupra performanţelor unui ciclu solar cogenerativ Joule Brayton de micã putere. Schema constructivã a motorului Joule Brayton a presupus sistemul: compresor centrifug – turbinã centripetã – captator/concentrator de radiaţie solarã– recuperator intern de cãldurã, ce poate fi utilizat pentru puteri mici. S-au considerat trei posibili agenţi de lucru, aer, azot şi dioxid de carbon. Pentru a obţine rezultate numerice cât mai veridice, schema numericã de calcul a considerat cãlduri specifice variabile, rapoarte de comprimare şi randamente izentropice corespunzãtoare tipurilor de compresor şi turbinã adoptate, diferite grade de concentrare a radiaţiei solare prin intermediul temperaturii maxime pe ciclu. Analiza numericã a evidenţiat cã alegerea unui agent de lucru trebuie fãcutã pentru fiecare aplicaţie în parte, în funcţie şi de condiţii restrictive specifice diferite de cele termodinamice, cum ar fi de exemplu raportul dintre fluxul termic cerut de consumatorii de cãldurã şi puterea furnizatã impusã de consumatorii acestei utilitãţi energetice, tehnologii de fabricaţie şi valoarea investiţiilor specifice, etc.
Cuvinte cheie: ciclu solar cogenerativ Joule Brayton, agenţi de lucru, performanţe termodinamice, schemã logicã de calcul.

Abstract. The paper includes a comparative analysis of the effect of the working fluid type upon the performances of a small solar cogeneration Joule Brayton cycle. The engine scheme considered the setup: radial compressor – centripetal turbine – concentrating solar power (CSP) heat exchanger – internal recovering heat exchanger – and external cogeneration heat exchanger. They were evaluated three working fluids, air, nitrogen, and carbon dioxide. The numerical code involved variable heat capacities, compression ratios and isentropic efficiencies typical for the chosen compressors and gas turbine, and various solar radiation concentrating degrees by the intermediary of the maximum temperature on the cycle. The numerical analysis emphasized that the choosing of a certain working fluid must follow also extra non-thermodynamically based real operational restrictive conditions, such as for instance the operational heat per power ratio, technological approaches and specific financial investments etc.
Keywords: solar cogeneration Joule Brayton cycle, working fluids, thermodynamic performances, numerical algorhytm.

1. INTRODUCTION

The next future of energy systems must deliberate on their structure including besides classical energy systems, fueled and nuclear, new advanced and more and more widespread renewable based ones.

These new systems are to be "standardized" by more points of view, for instance:
- thermodynamic criteria like power, first and second law efficiencies,
- technological methodologies adapted to small or large power systems, open for air or closed for other working fluids, compatible materials, design for assembling at the system operational start and disassembling at the system life end,
- financial issues as the specific investment,
- life cycle assessments, and so on.

This paper tried to find out if there are major effects of the working fluid nature upon the thermodynamic performances of the small solar Joule Brayton engines.

The numerical analysis emphasized that the choosing of a certain working fluid must follow also extra, non-thermodynamically based, real operational restrictive conditions, for instance the operational heat per power ratio, technological approaches and specific financial investments etc.

2. MATHEMATICAL ALGORHYTM

2.1. Hypotheses

The operational cycle is sketched in Figure 1. The successively processes are:

- 1 – 2r irreversible compression,
- 2r – 3r irreversible pre-heating by internal heat recovering,
- 3r – 4r irreversible heating by solar radiation,
- 4r – 5r irreversible expansion,
- 5r – 6r irreversible cooling by internal heat recovering,
- 6r – 7r irreversible cooling by cogeneration,
- 7r – 1 irreversible cooling by releasing out the exhaust heat.

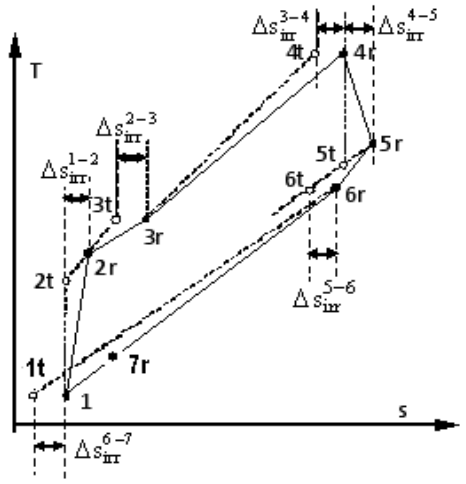

Fig. 1. The solar cogeneration Joule Brayton cycle

The adopted assumptions on the cycle are:

– the minimum temperature on the cycle
$T_1 = 293.15$ K;

– the maximum temperature on the cycle
T_{4r} =873.15 / 1073.15 / 1273.15 / 1473.15 K;

– compression ratios
$\pi_C = p_2/p_1 = 2.5 / 3.5 / 4.5$

– isentropic efficiencies
$\eta_C = 0.8$, $\eta_T = 0.8$;

– mechanical power loss: 1%;

– effectiveness of internal heat exchanger
$\varepsilon_{recov} = 0.95$;

– irreversible pressure drops by
$p_{3r}/p_{2r} = 0.98$, $p_{4r}/p_{3r} = 0.99$, $p_{6r}/p_{5r} = 0.970$,
$p_{6r}/p_{7r} = 0.955$, and $p_{7r}/p_1 = 0.9975$;

– heat capacities evaluated by polynomials of 4th order;

– ideal gas constants compiled as mean values of the difference between the constant pressure heat capacity and the constant volume heat capacity, on the range 20 – 1300 degrees Celsius.

2.2. Basic relations

♦ Heat capacities interpolated by polynomials:

$$c_p = a_0 + a_1 \cdot T + a_2 \cdot T^2 + a_3 \cdot T^3 + a_4 \cdot T^4$$
$$c_v = b_0 + b_1 \cdot T + b_2 \cdot T^2 + b_3 \cdot T^3 + b_4 \cdot T^4 \quad (1)$$

♦ Mean adiabatic exponents of reversible adiabatic process 1 – 2t and 4r – 5t:

$$\gamma_{12} = \frac{\int_{T_1}^{T_{2t}} c_p \cdot dT}{\int_{T_1}^{T_{2t}} c_v \cdot dT}, \quad \gamma_{45} = \frac{\int_{T_{4r}}^{T_{5t}} c_p \cdot dT}{\int_{T_{4r}}^{T_{2t}} c_v \cdot dT} \quad (2)$$

♦ Isentropic efficiencies of irreversible adiabatic process 1 – 2r and 4r – 5r:

$$\eta_C = \frac{\int_{T_1}^{T_{2t}} c_p \cdot dT}{\int_{T_1}^{T_{2r}} c_p \cdot dT}, \quad \eta_T = \frac{\int_{T_{4r}}^{T_{5r}} c_p \cdot dT}{\int_{T_{4r}}^{T_{5t}} c_p \cdot dT} \quad (3)$$

♦ Mean ideal gas constants over a temperature range, from T_{min} to T_{max}:

$$R = \frac{\int_{T_{min}}^{T_{max}} \left(c_p - c_v\right) \cdot dT}{T_{max} - T_{min}} \quad (4)$$

♦ Effectiveness of internal recovering heat exchanger, knowing that the flow heat capacity rate along the process 2r – 3t is smaller than that along the process 5r – 6t, since the specific heat capacity is larger while the temperature is larger:

$$\varepsilon_{recov} = \frac{\int_{T_{2r}}^{T_{3t}} c_p \cdot dT}{\int_{T_{2r}}^{T_{5r}} c_p \cdot dT} \approx \frac{T_{3t} - T_{2r}}{T_{5r} - T_{2r}} \quad (5)$$

♦ Pressures and temperatures:

$$p_1 = 1 \text{ bar}, \; p_{2t} = p_1 \cdot \pi_C, \; p_{2r} = p_{2t}, \; p_{3t} = p_{2r},$$
$$p_{3r} = 0.98 \cdot p_{3t}, \; p_{4r} = 0.99 \cdot p_{3r}, \quad (6)$$
$$p_{7r} = \frac{p_1}{0.9975}, \; p_{6r} = \frac{p_{7r}}{0.955}, \; p_{5r} = \frac{p_{6r}}{0.97}$$

$$T_1 = 293.15 \text{ K}, \; T_{3t} = T_{3r}, \; T_{4t} = T_{4r}, \; T_{6t} = T_{6r}, \quad (7)$$
$$T_{7r} = 363.15 \text{ K}$$

2.3. Basic numerical code equations

♦ Reversible adiabatic compression 1 – 2t:

$$T_{2t} = T_1 \cdot \left(\frac{p_{2t}}{p_1} \right)^{(\gamma_{12}-1)/\gamma_{12}} \quad (8)$$

Solving this equation by an iterative method, e.g. trial and error, it yields the temperature T_{2t}.

- Irreversible adiabatic compression 1 – 2r:

$$\eta_C \cdot \int_{T_1}^{T_{2r}} c_p \cdot dT = \int_{T_1}^{T_{2t}} c_p \cdot dT \quad (9)$$

By using also an iterative method, from this equation it results T_{2r}.

- Reversible adiabatic expansion 4r – 5t:

$$T_{5t} = T_{4r} \cdot \left(\frac{p_{5t}}{p_{4r}} \right)^{(\gamma_{45}-1)/\gamma_{45}} \quad (10)$$

From this equation it yields the temperature T_{5t}, by means of an iterative method, e.g. trial and error.

- Irreversible adiabatic expansion 4r – 5r:

$$\eta_T \cdot \int_{T_{4r}}^{T_{5t}} c_p \cdot dT = \int_{T_{4r}}^{T_{5r}} c_p \cdot dT \quad (11)$$

A similar way of solving this equation, it obtains T_{5r}.

- Internal heat recovering (3r – 4t) + (5r – 6t):

$$T_{3t} = \varepsilon_{recov} \cdot (T_{5r} - T_{2r}) + T_{2r}\,,\ T_{3r} = T_{3t} \quad (12)$$

$$\int_{T_{2r}}^{T_{3t}} c_p \cdot dT = -\int_{T_{5r}}^{T_{6t}} c_p \cdot dT\,,\ T_{6r} = T_{6t} \quad (13)$$

In equation (11) we impose ε_{recov}, and thus it obtains T_{3t}. The equation (12) can be solved numerically by an iterative method and gives T_{6t}.

- Specific powers interactions:

$$w_C = -\int_{T_1}^{T_{2r}} c_p \cdot dT \quad (14)$$

$$w_T = -\int_{T_{4r}}^{T_{5r}} c_p \cdot dT \quad (15)$$

$$w_{cycle} = w_T + w_C\,,\ w_{supplied} = 0.99 \cdot w_{cycle} \quad (16)$$

- Specific heat rate interactions:

$$q_{solar} = \int_{T_{3r}}^{T_{4t}} c_p \cdot dT \quad (17)$$

$$q_{cog} = \int_{T_{6r}}^{T_{7r}} c_p \cdot dT \quad (18)$$

$$q_{exhaust} = \int_{T_{7r}}^{T_1} c_p \cdot dT \quad (19)$$

- First law efficiencies:

$$\eta_w = \frac{w_{supplied}}{q_{solar}} \quad (20)$$

$$\eta_{cog} = \frac{w_{supplied} + q_{cog}}{q_{solar}} \quad (21)$$

3. NUMERICAL RESULTS

The numerical results are shown in Figures 2 to 10.

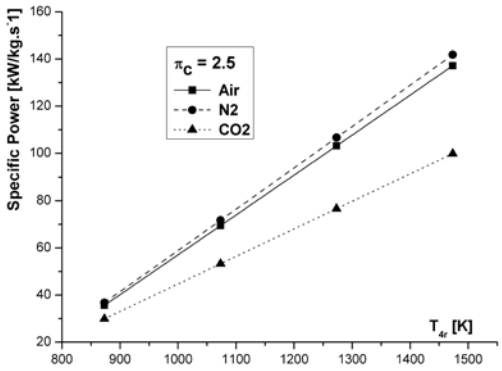

Fig. 2. Specific power versus maximum temperature on the cycle. $\pi_C = 2.5$

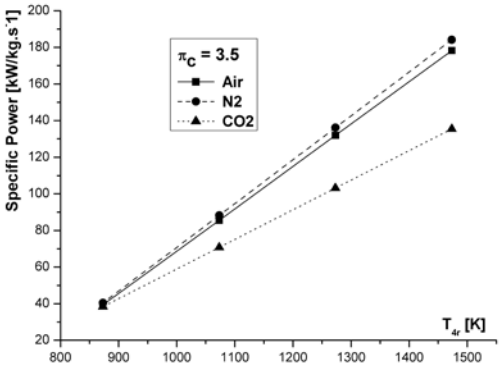

Fig. 3. Specific power versus maximum temperature on the cycle. $\pi_C = 3.5$

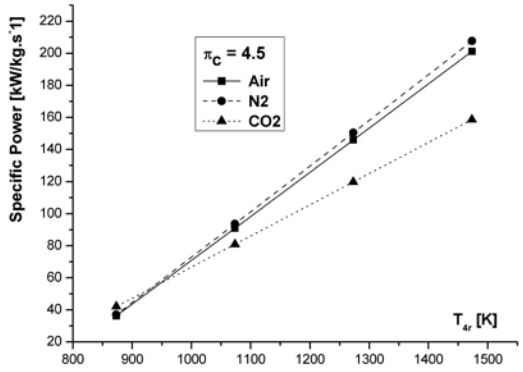

Fig. 4. Specific power versus maximum temperature on the cycle. $\pi_C = 4.5$

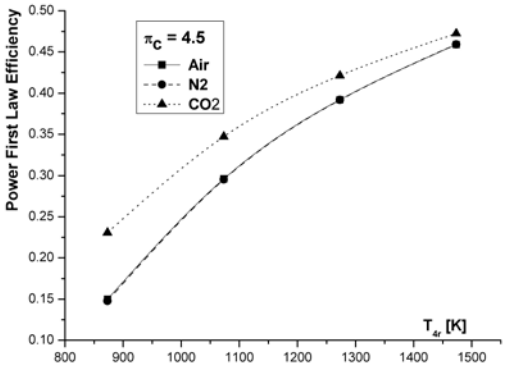

Fig. 7. Power first law efficiency versus maximum temperature on the cycle. $\pi_C = 4.5$

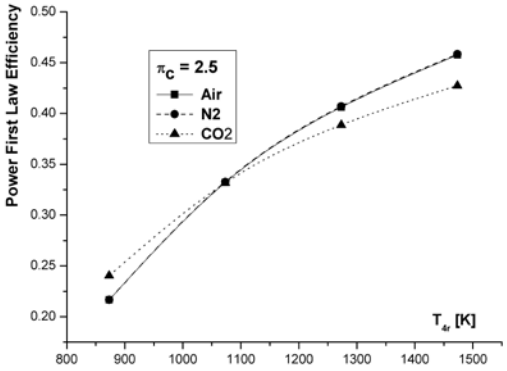

Fig. 5. Power first law efficiency versus maximum temperature on the cycle. $\pi_C = 2.5$

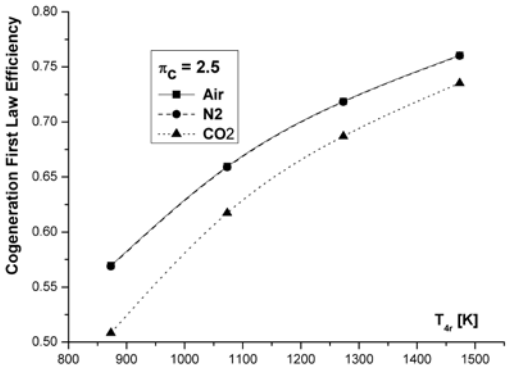

Fig. 8. Cogeneration first law efficiency versus maximum temperature on the cycle. $\pi_C = 2.5$

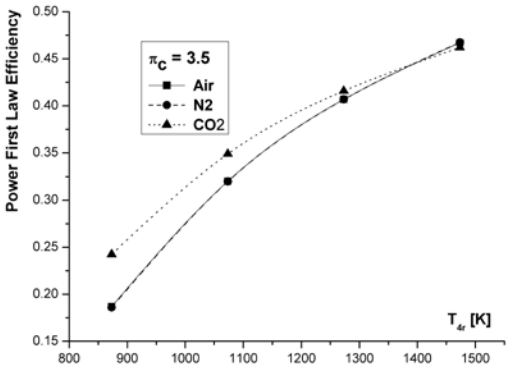

Fig. 6. Power first law efficiency versus maximum temperature on the cycle. $\pi_C = 3.5$

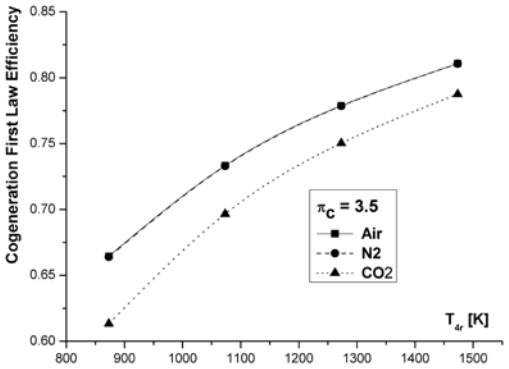

Fig. 9. Cogeneration first law efficiency versus maximum temperature on the cycle. $\pi_C = 3.5$

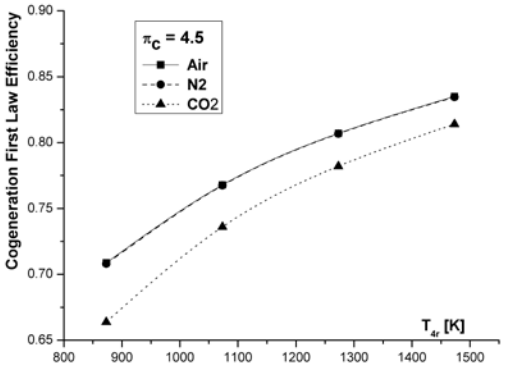

Fig. 10. Cogeneration first law efficiency versus maximum temperature on the cycle. $\pi_C = 4.5$

4. CONCLUSIONS

The numerical results revealed that the nature of the working fluid is controlling the performances of the solar cogeneration cycle. At a first look, we cannot say which working fluid is more appropriate to solar applications.

The main conclusions emphasize that:

- the air and nitrogen are quite similar in effects on the specific power and the first law efficiencies,
- the specific power supplied by the carbon dioxide is smaller that those supplied by air and nitrogen,
- the power first law efficiencies of carbon dioxide really can compete with those of air/nitrogen, especially at larger compression ratios and at lesser T_{4r},
- for the carbon dioxide, the cogeneration first law efficiencies are smaller than those for air and nitrogen; the cogeneration first law efficiencies might be actually compared in a specific solar application, when the ratio of cogenerated heat to supplied power is imposed by customers.

REFERENCES

[1] Gheorghe Dumitrascu, Aristotel Popescu – *Influence of Working Fluid Properties on Internal Irreversibility of Power Systems*. IMECE2010 – 40467, Proceedings of the ASME 2010 International Mechanical Engineering Congress & Exposition, November 12-18, 2010, Vancouver, British Columbia, Canada

[2] Lingen Chen, Wanli Zhang, Fengrui Sun – *Power, efficiency, entropy-generation rate and ecological optimization for a class of generalized irreversible universal heat-engine cycles*. Applied Energy 84 (2007) 512–525

[3] S.K. Tyagi, G.M. Chen, Q. Wang, S.C. Kaushik – *Thermodynamic analysis and parametric study of an irreversible regenerative-intercooled-reheat Brayton cycle.* International Journal of Thermal Sciences 45 (2006) 829–840

[4] Wanli Zhang, Lingen Chen, Fengrui Sun – *Power and efficiency optimization for combined Brayton and inverse Brayton cycles.* Applied Thermal Engineering 29 (2009) 2885–2894

Muzeul Olteniei din Craiova reuneste mai multe institutii muzeale create si dezvoltate de la începutul sec. al XIX-lea si pina astazi.
Sediul central al Muzeului Olteniei se afla în cladirea monumentala, din str. Popa Sapca nr.4, proiectata de cunoscutul arhitect C. Iotu si construita, începind din anul 1920 de firmele de constructii Dalla Barba si Peressutti. Palatul "Ramuri" cum este cunoscut edificiul se afla în centrul municipiului Craiova, între Palatul Jean Mihail, azi Muzeul de Arta, Colegiul Carol I si Biserica Sfinta Treime, ctitorie a familiei princiare Barbu Stirbei si Palatul Prefecturii Judetului Dolj proiectat de arhitect P. Antonescu.